Trapping of active Brownian and run-and-tumble particles: A first-passage time approach

Emily Qing Zang Moen [1], Kristian Stølevik Olsen [2], Jonas Rønning [1], and Luiza Angheluta [1]

[1]*The Njord Center, Department of Physics, University of Oslo, Blindern, 0316 Oslo, Norway*
[2]*Nordita, Royal Institute of Technology and Stockholm University, Hannes Alfvéns väg 12, 23, 106 91 Stockholm, Sweden*

We use a first-passage time approach to study the statistics of the trapping times induced by persistent motion of active particles colliding with flat boundaries. The angular first-passage time distribution and mean first-passage time are calculated exactly for active Brownian and run-and-tumble particles, and the results of the two prototypes of active particles are contrasted. Theoretical predictions are in excellent agreement with Langevin simulations of active particle dynamics. Our results shed further light on how active particles with different dynamics may have equivalent statistical properties in the bulk yet behave differently near boundaries or obstacles.

I. INTRODUCTION

Active matter is a class of nonequilibrium systems in which the constituents are self-propelled by consuming energy from their environment. Much of the theoretical interest in the field comes from the diverse emergent phenomena with no counterparts in analogous equilibrium or passive systems. The role of disorder and confinement has attracted particular attention since they are present in most realistic active matter systems, like those found in biological matter, and also due to potential microfluidic applications. A myriad of studies have revealed the importance of boundaries in shaping the macroscopic behavior of active systems [1], including novel collective states in solid confinement [2,3] and surface accumulation and currents [4–6].

In this paper, we study the statistical features of trapping induced by persistent motion of active particles near a flat, solid boundary. As limit cases, we compare the statistics of trapping times corresponding to active Brownian particles (ABPs) and run-and-tumble particles (RTPs). While these two minimal models are well known to give rise to the same statistical properties in open spaces [7], we show through analytical calculations and numerical simulations that the two differ significantly under confinement, where the microscopic details of persistent motion become important for the wall-trapping statistics. This is relevant for phenomena like surface accumulation and also, for example, in studies of activity-induced pressure, which depends on particle-boundary contact times. Previous works have also reported different behaviors of ABPs and RTPs in confinement. For example, in a harmonic confinement, the ABPs tend to drift more around the high-

potential regions of the potential than RTPs [8]. It has also been shown that the two particle types separate when released inside a mazelike geometry [9]. This separation was also attributed to the difference in surface interactions. The surface residence time was studied for a modified run-and-tumble model and compared with *Escherichia coli* data in Ref. [10], and the effect of hydrodynamic interactions on the residence times of ABPs was studied in Ref. [11]. However, there is a subtlety in how the residence time is defined and how it impacts the residence time statistics. In previous works, the residence time was typically calculated by introducing a boundary layer with an *ad hoc* width and measuring the time spent by the active particle within that layer. We here propose an alternative way to determine the trapping time that is suitable for the case of simple steric body forces between the particle and boundary. Namely, we define the trapping as the time that the particle *effectively* exchanges momentum with the wall. In other words, here we consider the trapping time to be the time that the particle resides at the wall with a nonzero velocity normal to the wall. Figure 1 illustrates trapping events of both ABPs and RTPs in a box.

In a minimal stochastic model, the two-dimensional (2D) dynamics of an active particle is typically described by following stochastic equations [12]:

$$\dot{\mathbf{x}} = v_0 \hat{\mathbf{e}}(t) + \mathbf{F}_c, \tag{1}$$

$$\dot{\theta} = \sqrt{2D_r}\xi(t) + \sum_\alpha \Delta\theta_\alpha \delta(t - t_\alpha). \tag{2}$$

Here v_0 is the constant self-propulsion speed, D_r is the rotational diffusivity, and t_α are random tumbling times generated by a Poisson process with rate γ. Here $\Delta\theta_\alpha$ are uniform random angles describing the tumbling angle. The case $D_r = 0$ yields pure run-and-tumble particles, while $\gamma = 0$ results in active Brownian motion. These are the two cases that we consider separately. The confinement force $\mathbf{F}_c$ is taken to be a
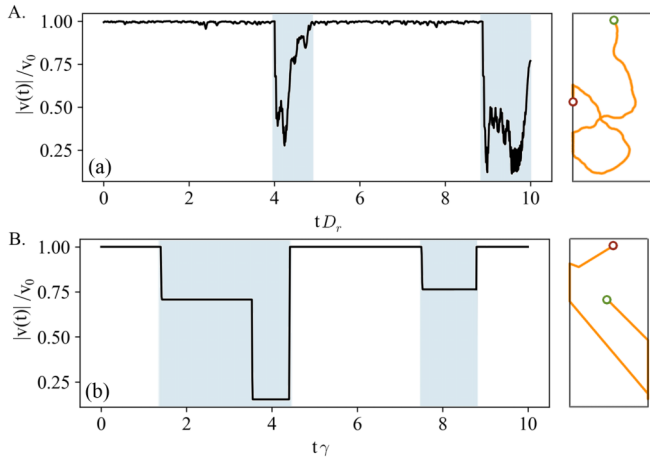
FIG. 1. Sketch of the system under consideration, where (a) active Brownian particles and (b) run-and-tumble particles collide and get trapped at solid flat boundaries (rightmost plots). The speed time series shows trapping times as periods of reduced self-propulsion compared to bulk motion. Trapping durations are indicated by blue shaded regions.

purely steric body force, modeled as

$$\mathbf{F}_c = \begin{cases} -v_0(\hat{\mathbf{e}} \cdot \hat{\mathbf{n}})\hat{\mathbf{n}} & \text{at the boundary,} \\ 0 & \text{in bulk,} \end{cases} \quad (3)$$

where $\hat{\mathbf{n}}$ is the outward unit vector of the wall boundary. Such steric boundary interactions do not induce any torques on the particle's direction of motion, so that the angular dynamics remains the same both at the boundary and in the bulk. Additional boundary effects on the angular dynamics may be realistic if hydrodynamic interactions are taken into account or if the particles in question have a nonspherical elongated shape [13,14]. Different kinds of migrating cells or swimming bacteria display various scattering behaviors from surfaces [15,16]. We focus primarily on the effect of persistent motion into flat walls of pointwise active particles and aim to understand the effect of the two different types of angular dynamics on wall-trapping statistics.

Our approach is to map the problem of finding the trapping duration to a first-passage problem for the marginalized angular dynamics for active Brownian particles ($\gamma = 0$) and run-and-tumble particles ($D_r = 0$). This angular first-passage time (FPT) distribution is calculated straightforwardly from the relation to the survival probability $S(t, \theta_a|\theta_0)$. This is the probability that the angular stochastic process remains inside an angular domain $(-\theta_a, \theta_a)$ up to time t given an initial angle θ_0. By solving the corresponding Fokker-Planck or master equation for the angular distributions $\rho_a(\theta, t|\theta_0)$ conditioned on some incoming angle θ_0 and with absorbing boundary conditions at the target angles $\pm\theta_a$, we can then compute the survival probability by

$$S(t, \theta_a|\theta_0) = \int_{-\theta_a}^{\theta_a} d\theta \, \rho_a(\theta, t|\theta_0), \quad (4)$$

which is also conditioned on the incoming angle. On the other hand, we can also write the survival distribution as the probability that the target angle θ_a is reached for the first time

at time t; thus [17],

$$S(t, \theta_a|\theta_0) = 1 - \int_0^t d\tau F(\tau, \theta_a|\theta_0), \quad (5)$$

where $F(\tau, \theta_a|\theta_0)$ is the FPT probability density which follows from knowing the survival distribution using the equation above as

$$F(t, \theta_a|\theta_0) = -\frac{d}{dt} S(t, \theta_a|\theta_0). \quad (6)$$

In more realistic situations where a particle encounters a boundary, the collision angle or incoming angle θ_0 will be random, meaning we should interpret $S(t, \theta_a|\theta_0)$ as a conditional probability on the random incoming angle. For a given distribution $\mathcal{P}(\theta_0)$ of incoming angles, we may integrate out this random variable, resulting in the averaged FPT distribution

$$\overline{F}(t, \theta_a) = \int_{-\theta_a}^{\theta_a} d\theta_0 F(t, \theta_a|\theta_0) \mathcal{P}(\theta_0). \quad (7)$$

Similarly, we may calculate the conditional mean FPT $T_1(\theta_a|\theta_0)$ and then integrate over the incoming angles to obtain

$$\overline{T}_1(\theta_a) = \int_{-\theta_a}^{\theta_a} d\theta_0 T_1(\theta_a|\theta_0) \mathcal{P}(\theta_0) \quad (8)$$

$$= \int_0^\infty dt \overline{F}(t, \theta_a) t. \quad (9)$$

From the perspective of the first-passage problem, the incoming angle of a particle when colliding with the boundary is, in essence, an initial condition, and we may refer to it as such in the following. We, however, note that it is the same as the initial conditions of the particle itself, which we always initialize far from the boundary.

The types of averages discussed above may dramatically alter the analytical form of the FPT distribution, as observed recently in the first-passage problem of a Brownian process with a single target and normally distributed initial conditions [18]. Here it was observed that as the width of the distribution of the initial conditions was varied, the FPT distribution underwent a transition from monotonic to nonmonotonic at a certain critical width. In the case of ABPs, where the angular dynamics is Brownian, a distribution of incoming angles can significantly change the FPT distribution. As we will discuss below, however, this is not the case for RTPs.

The remainder of this paper is structured as follows. In Sec. II A, we consider the relevant class of first-passage problems for the rotational dynamics of a run-and-tumble particle, namely, the statistics of the first passage out of the angular domain $(-\theta_a, \theta_a)$. The case of trapping at a flat wall is obtained by setting $\theta_a = \pi/2$. Simple arguments based only on the Poissonian nature of tumbles leads to a simple analytical expression for the trapping time distribution in both two and three dimensions. Furthermore, the first-passage time distribution and the corresponding mean have no dependence on the incoming angle of the particles and are hence insensitive to the distribution of incoming angles. Section II B considers the active Brownian case in two dimensions. As the marginalized angular dynamics is Brownian, an exact analytical solution is readily obtainable. Upon averaging over incoming angles, various distribution shapes can be found. Section III discusses
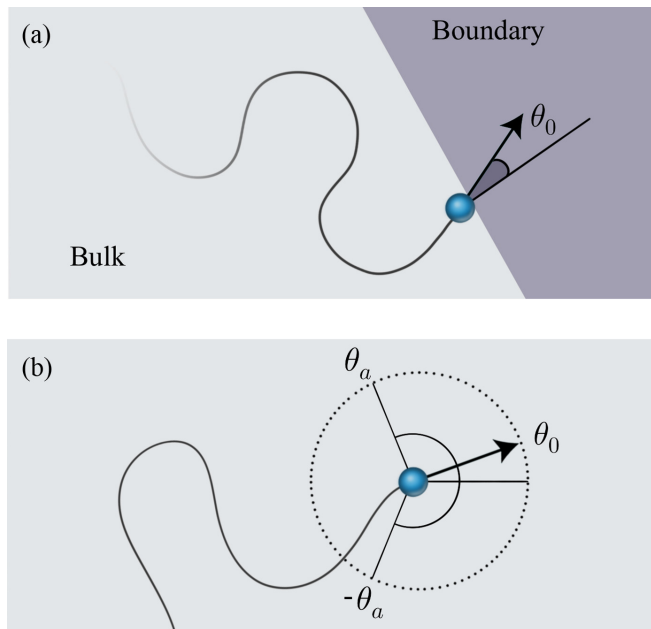
FIG. 2. (a) Active particles colliding with a flat boundary with an incoming angle θ_0. (b) General angular first-passage problem with arbitrary target angle θ_a.

ABPs and RTPs confined to a 2D infinite channel. Comparisons of the analytical results and numerical simulations are made, showing excellent agreement. Section IV provides a concluding discussion and potential outlooks.

II. THE FIRST-PASSAGE PROBLEM

The class of first-passage problems we are considering is based on the survival of a stochastic angular variable in the angular domain $(-\theta_a, \theta_a)$, with absorbing boundary point $\theta_a \leqslant \pi$. As discussed above, the case $\theta_a = \pi/2$ corresponds to the escape from a flat wall. In this setup, we use a convention so that a particle that collides head-on with a boundary has an incoming angle $\theta_0 = 0$. See Fig. 2 for an illustration showing the conventions. We first solve the problem for run-and-tumble particles and then proceed to the active Brownian case.

A. Run-and-tumble case

For run-and-tumble particles, the angular variable performs discontinuous jumps on the circle at random times that obey Poisson statistics. This is therefore equivalent to a discrete random walk on the circle with arbitrarily large (but periodic) step sizes. Moreover, the absorbing targets are not point sinks but rather extended regions, similar to those in the recent study in Ref. [19].

To calculate the survival probability, we assume that in the interval $(0, t)$ there are exactly $N_{\text{tum}}(t) = n$ tumbles,

$$\theta_0 \rightarrow \theta_1 \rightarrow \theta_2 \rightarrow \theta_3 \rightarrow \cdots \rightarrow \theta_n. \tag{10}$$

The probability that this happens is simply given by the Poisson probability $P[N_{\text{tum}}(t) = n] = \exp(-\gamma t)(\gamma t)^n/n!$. To find the survival probability that the angle remains inside a domain $(-\theta_a, \theta_a)$ during these tumbles, we note that the tumbles are

independent and equivalent to uniformly picking a random point on the circle. Hence, the survival probability conditioned on a fixed number of tumbles is simply

$$S_n(t, \theta_a | \theta_0) = \Theta(\theta_a - |\theta_0|)P[N_{\text{tum}}(t) = n]\left(\frac{\theta_a}{\pi}\right)^n. \tag{11}$$

Here θ_a/π is the probability that a single tumble remains in $(-\theta_a, \theta_a)$, and the Heaviside theta function ensures that the survival probability is zero if the initial angle is outside the domain of interest. The survival probability in time t is then obtained by marginalizing over the number of tumbles,

$$S(t, \theta_a | \theta_0) = \sum_{n=0}^{\infty} S_n(t, \theta_a | \theta_0) \tag{12}$$

$$= \Theta(\theta_a - |\theta_0|)e^{-\gamma\left(1 - \frac{\theta_a}{\pi}\right)t}. \tag{13}$$

Here we used Eq. (11) for S_n, as well as the series for the exponential function. From Eq. (6), we can easily calculate the exponential FPT distribution

$$F(t, \theta_a | \theta_0) = \Theta(\theta_a - |\theta_0|)\gamma\left(1 - \frac{\theta_a}{\pi}\right)e^{-\gamma\left(1 - \frac{\theta_a}{\pi}\right)t}, \tag{14}$$

and we calculate its mean as

$$T_1(\theta_a | \theta_0) = \frac{\Theta(\theta_a - |\theta_0|)}{\gamma\left(1 - \frac{\theta_a}{\pi}\right)}. \tag{15}$$

Interestingly, the mean has a divergence as $\theta_a \rightarrow \pi$. This makes sense, as the probability of tumbling out of the domain $(-\theta_a, \theta_a)$ vanishes in this limit, and hence, we should expect an infinite first-passage time. To verify this result, we perform stochastic simulations of the tumbling dynamics and show in Fig. 3 that the dependence on θ_a of the mean first-passage time is in excellent agreement with the theoretical prediction.

The case corresponding to trapping at a flat boundary $\theta_a = \pi/2$ results in

$$F(t, \pi/2 | \theta_0) = \Theta\left(\frac{\pi}{2} - |\theta_0|\right)\frac{\gamma}{2}e^{-\gamma t/2}. \tag{16}$$

Assuming that $|\theta_0| < \theta_a$, we can ignore the Heaviside step function in the above expressions. In this case there is no remaining dependence on the collision angle θ_0, and hence,
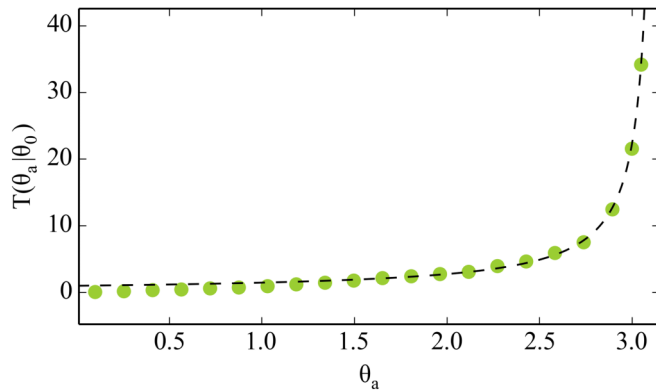

FIG. 3. Mean FPT in units of the persistence time as a function of target angle θ_a for the RTP case, showing clear agreement between theory (dashed line) and simulations (dots).

we have trivially that

$$\overline{F}(t, \theta_a) = F(t, \theta_a | \theta_0), \tag{17}$$

with similar notation for the mean FPT. This behavior originates in the fact that run-and-tumble dynamics is described by uniform transition probabilities. In the more general case, where tumbling angles follow a distribution, we expect the collision angle to play a more prominent role.

The above arguments generalize trivially to any stochastic search process in which space is sampled randomly and uniformly at times following a Poisson process. In particular this means that in the case of three dimensions, where the direction of motion is given by a point on a unit sphere, the FPT distribution is similarly given as

$$F_{3d}(t, \mathcal{D} | \theta_0) = \gamma \left(1 - \frac{|\mathcal{D}|}{4\pi}\right) e^{-\gamma\left(1 - \frac{|\mathcal{D}|}{4\pi}\right)t}, \tag{18}$$

where $\mathcal{D} \subset \mathbf{S}^2$ is the domain on the unit sphere out of which we are interested in tumbling and 4π is the sphere's total area. When an active particle is trapped at a two-dimensional boundary, the escape takes place when the director leaves the upper half sphere. In this case $|\mathcal{D}| = 2\pi$, and the FPT distribution reads

$$\overline{F}_{3d}(t) = \frac{\gamma}{2} e^{-\gamma t/2}. \tag{19}$$

The same argument extends to a d-dimensional particle trapped at a $(d-1)$-dimensional hypersurface, and in this sense the distribution is universal in $d \geqslant 2$. Alternatively, one can obtain the new direction of motion after a tumble by picking a uniformly random point on a d-dimensional sphere. This is typically done by generating a length d vector of standard normal variables. Upon normalization this vector points to a uniformly random point on the sphere. A RTP will be able to escape from the wall when *a single* one of these d normal variables changes time, which happens with rate $\gamma/2$ when tumbles take place at rate γ. Hence, the above FPT distribution is universal for all dimensions, and we will refer to it simply as $\overline{F}(t)$.

B. Active Brownian case

In contrast to the run-and-tumble case, the angular dynamics of an active Brownian particle is continuous and Brownian and can be solved using standard Fokker-Planck methods. The full dynamics of the distribution $P(\vec{x}, \theta, t)$ is, in general, described by a Fokker-Planck equation of the form

$$\partial_t P + v_0 [\hat{e}(\theta) \cdot \boldsymbol{\nabla}_x] P = D_r \partial_\theta^2 P, \tag{20}$$

where $\hat{e}(\theta) = [\cos\theta, \sin\theta]$ is the unit vector in the direction of motion of the particles in which they move with constant speed v_0. Marginalizing over the spatial variable $\rho = \int d\vec{x} P$ results simply in the diffusion equation $\partial_t \rho = D_r \partial_\theta^2 \rho$. Since the process is terminated before the angles have explored the full circle, no effects of periodicity are present in this calculation, and the problem is equivalent to that of normal Brownian motion on an interval. This classical problem was first studied in the 1950s by Darling and Siegert and has since then appeared in multiple references with various generalizations [17,20–24]. A standard approach to obtaining first-passage

times for such processes is to find the Laplace transform of the survival probability by means of a backward Fokker-Planck equation. From this the mean FPT is easily obtained. Another approach uses the well-known fact that Fokker-Planck equations of the type $\partial_t P = \mathcal{L}_{\text{FP}} P$ imply that the mean FPT satisfies $\mathcal{L}_{\text{FP}}^\dagger T_1 = -1$, evaluated at the initial condition [25]. In the diffusive case this is simply a boundary value problem for the Poisson equation. In either case, the mean FPT is known to take the quadratic form [17,24]

$$T_1(\theta_a | \theta_0) = \frac{\theta_a^2 - \theta_0^2}{2D_r}. \tag{21}$$

The aforementioned approaches, either by means of Laplace transforms or the Poisson equation, allow one to easily obtain the mean FPT directly from the Fokker-Planck equation. However, here we are also interested in the analytical form of the first-passage time distribution. We therefore directly solve the Fokker-Planck equation by means of an eigenfunction expansion and derive an expression for the mean FPT conditioned on an initial angle. This expression may then be used when we average over the distribution of initial angles.

We solve the rotational diffusion problem

$$\partial_t \rho_a(\theta, t) = D_r \partial_\theta^2 \rho_a(\theta, t), \quad \rho_a(\pm\theta_a, t) = 0, \tag{22}$$

with the initial condition being a Dirac delta function $\rho_a(\theta, 0) = \delta(\theta - \theta_0)$ located at an initial angle θ_0 that, like in the run-and-tumble case, is assumed to lie somewhere between the two absorbing angles. The solution to the above boundary value problem can be expressed as a series,

$$\rho_a(\theta, t) = \sum_{n=1}^{\infty} a_n(t) \psi_n(\theta) \tag{23}$$

$$= \sum_{n=1}^{\infty} a_n(t) \sin\left(\frac{n\pi(\theta - \theta_a)}{2\theta_a}\right), \tag{24}$$

where $\psi_n(\theta)$ are eigenfunctions of the Dirichlet Laplacian forming a complete basis for the function in the domain $(-\theta_a, \theta_a)$. Insertion into the diffusion equation gives the time evolution of the time-dependent coefficients as $a_n(t) = a_n(0) \exp[-D_r(n\pi/2\theta_a)^2 t]$. Through the orthogonality of the eigenfunctions we can find the remaining coefficients $a_n(0)$ from the initial condition as

$$a_n(0) = \frac{1}{\theta_a} \int_{-\theta_a}^{\theta_a} d\theta \, \rho_a(\theta, 0) \psi_n(\theta). \tag{25}$$

For a Dirac delta initial condition located at $\delta(\theta - \theta_0)$, the initial coefficients are simply $a_n(0) = \psi_n(\theta_0)/\theta_a$, giving the solution

$$\rho_a(\theta, t) = \frac{1}{\theta_a} \sum_{n=1}^{\infty} e^{-D_r\left(\frac{n\pi}{2\theta_a}\right)^2 t} \psi_n(\theta_0) \psi_n(\theta). \tag{26}$$

In the case of a Brownian process on the real line with a single absorbing target, the image method is a popular method used to satisfy the boundary conditions. The present case can also be solved using this method by appropriately placing image densities on either side of the absorbing angles $\pm\theta_a$. For each of these image densities to have the correct behavior, they will again need image densities of their own. This leads
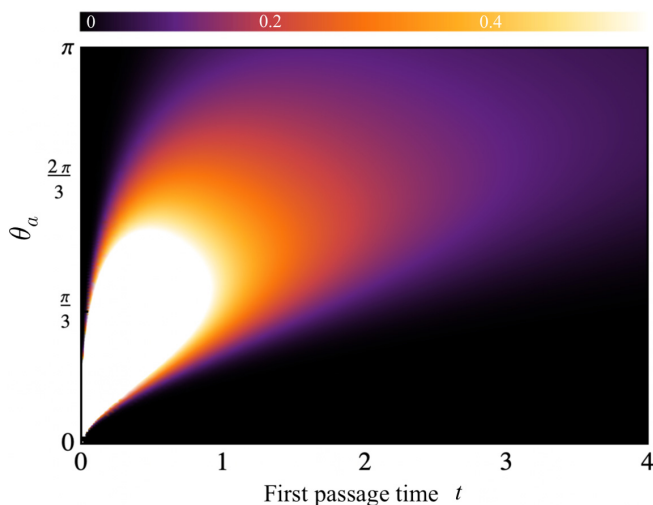
FIG. 4. Plot showing the FPT distribution as a function of passage times t and target angle θ_a, using Eq. (28). Here $\theta_0 = 0$ for simplicity.

to an infinite sum over densities and their images, which is equivalent to the above solution.

To obtain the survival probability, we use Eq. (4) together with the solution in Eq. (26). When integrating over the domain $(-\theta_a, \theta_a)$, we first note that the even terms in Eq. (26) will vanish since $\psi_{2n}(\theta)$ are functions of odd parity. Integrating the remaining odd terms in Eq. (26) results in the survival probability

$$S(t, \theta_a|\theta_0) = \frac{2}{\theta_a} \sum_{n=0}^{\infty} (-1)^n \frac{1}{\mu_n} \cos(\mu_n \theta_0) e^{-D_r \mu_n^2 t}, \qquad (27)$$

where we have introduced $\mu_n = (2n+1)\pi/(2\theta_a)$ for notational simplicity. The corresponding infinite series for the FPT distribution then follows as

$$F(t, \theta_a|\theta_0) = \frac{2D_r}{\theta_a} \sum_{n=0}^{\infty} (-1)^n \mu_n \cos(\mu_n \theta_0) e^{-D_r \mu_n^2 t} \quad (28)$$

$$= \frac{D_r}{\theta_a} \frac{d}{d\theta_0} \vartheta_1 \left(e^{-D_r \pi^2 t/\theta_a^2}, \frac{\pi \theta_0}{2\theta_a} \right), \qquad (29)$$

where we used the elliptic theta $\vartheta_1(q, z) = 2\sum_{n=0}^{\infty} (-1)^n q^{(n+1/2)^2} \sin[(2n+1)z]$ (see, e.g., Ref. [26]). Figure 4 shows a color map of the FPT probability density. We see that for small target angles the distribution is sharply peaked at small times. For larger target angles there is a maximum in the FPT distribution as a function of passage time (horizontal sections), representing the typical passage time; it is rare that the angular process finds the target quicker than at this peak, and it is also rare that the process remains in the bulk of $(-\theta_a, \theta_a)$ for longer times. These rare cases where the particle remains trapped in some angular domain for a long time contribute to the tail of the FPT distribution. From Eq. (28) we can see that with the large-t behavior the distribution becomes exponential, with $F(t, \theta_a|\theta_0) \sim \exp(-D_r \mu_0^2 t)$. Notice that this exponential tail behavior is different from the pure exponential behavior found in the RTP case.

We can also verify that the distribution in Eq. (28) is normalized. We note that by definition $\int_0^\infty dt F(t, \theta_a|\theta_0) = S(0, \theta_a|\theta_0)$, where we used $S(\infty, \theta_a|\theta_0) = 0$. Therefore, we have

$$\int_0^\infty dt F(t, \theta_a|\theta_0) = S(0, \theta_a|\theta_0) \qquad (30)$$

$$= \frac{2}{\theta_a} \sum_{n=0}^{\infty} (-1)^n \frac{\cos(\mu_n \theta_0)}{\mu_n}, \qquad (31)$$

which takes a form similar to the series expansion of the arctangent. Expressing the cosine as the sum of complex exponentials and using the identity $\tan^{-1}(e^{ix}) + \tan^{-1}(e^{-ix}) = \pi/2$ for $|x| < \pi/2$, we verify that the sum evaluates to unity for all θ_0.

Now, we want to check that our FPT distribution has a mean with the same quadratic dependence on θ_a as in Eq. (21). The mean FPT as a function of θ_a and conditioned on the incoming angle θ_0 can be calculated directly as the first moment of the FPT distribution, namely,

$$T_1(\theta_a|\theta_0) = \int_0^\infty dt\, t F(t, \theta_a|\theta_0). \qquad (32)$$

Using this expression in Eq. (28), we find the mean FPT expressed as the infinite series

$$T_1(\theta_a|\theta_0) = \frac{2}{D_r \theta_a} \sum_{n=0}^{\infty} (-1)^n \frac{\cos(\mu_n \theta_0)}{\mu_n^3}. \qquad (33)$$

To make the connection to Eq. (21) clear, we note that this is an analytical function of θ_0 and thus has a well-defined Taylor series expansion given as

$$T_1(\theta_a|\theta_0) = \sum_{k=0}^{\infty} \left\{ \frac{2}{D_r \theta_a} \sum_{n=0}^{\infty} (-1)^{n+k} \frac{\mu_n^{2k-3}}{(2k)!} \right\} \theta_0^{2k}.$$

Here it is worth noting that the series representation of the Taylor coefficients, given by the expression in the brackets, is divergent for $k \geqslant 2$ since μ_n grows linearly in n. However, regularization schemes like Abel summation can be used to assign a value of zero to all these higher-order coefficients, leaving only the first two terms nonzero. This results in the quadratic expression

$$T_1(\theta_a|\theta_0) = \frac{\theta_a^2 - \theta_0^2}{2D_r}, \qquad (34)$$

which is the classical result (21), as expected. This simple parabolic form tells us that for a fixed target angle θ_a, the initial angle $\theta_0 = 0$ always maximizes the mean FPT. Physically, particles that collide with a solid wall head-on are, on average, trapped for the longest time, as one would expect. However, the incoming angle should be considered random in realistic scenarios.

When averaging over a distribution $\mathcal{P}(\theta_0)$ of initial angles, we note that the FPT distribution takes the general form of an infinite series given by the superposition of exponential time

decays with different coefficients,

$$\overline{F}(t, \theta_a)$$

$$= \frac{2D_r}{\theta_a} \sum_{n=0}^{\infty} (-1)^n \mu_n \left(\int d\theta_0 \mathcal{P}(\theta_0) \cos(\mu_n \theta_0) \right) e^{-D_r \mu_n^2 t}. \quad (35)$$

To proceed, we note that the collision angles θ_0 when an active particle encounters a flat boundary can never be at $\pm\pi/2$, as this corresponds to motion parallel to the boundary. In the context of the present first-passage problem with general target angle θ_a, this corresponds to imposing absorbing boundary conditions $\mathcal{P}(\pm\theta_a) = 0$. Since the particles are achiral, we also expect by symmetry that $\mathcal{P}(\theta_0)$ is an even function. Combined, these facts imply that we can write the distribution of incoming angles as the cosine series

$$\mathcal{P}(\theta_0) = \sum_n \tilde{\mathcal{P}}_n \cos(\mu_n \theta_0), \quad (36)$$

with coefficients determined by the orthogonality condition

$$\int d\theta_0 \mathcal{P}(\theta_0) \cos(\mu_n \theta_0) = \theta_a \tilde{\mathcal{P}}_n. \quad (37)$$

Thus, the final expression for the collision-averaged FPT distribution can be written equivalently in terms of the coefficients $\tilde{\mathcal{P}}_n$ as

$$\overline{F}(t, \theta_a) = 2D_r \sum_{n=0}^{\infty} (-1)^n \mu_n \tilde{\mathcal{P}}_n e^{-D_r \mu_n^2 t}. \quad (38)$$

It is worth noting that averaging over collisions will not affect the tail (long trapping-time limit) of the distribution, which is dominated by the first term of the series $\overline{F} \sim \exp(-D_r \mu_0^2 t)$, and rather influences only its behavior at short trapping times. This is sensible also intuitively, as the particles that contribute to the tail of the distribution are those that spend a long time finding any of the absorbing targets and hence no longer remember their initial collision angle. The short passage times are determined by the collision angle distribution, and by changing the coefficients $\tilde{\mathcal{P}}_n$ one can observe both monotonic and nonmonotonic behaviors in $\overline{F}$. Different distributions $\mathcal{P}(\theta_0)$ can, in principle, be constructed by experimentally or numerically considering various setups for releasing the particles near a flat boundary. In addition, we find the averaged mean FPT as

$$\overline{T}(\theta_a) = \frac{2}{D_r} \sum_{n=0}^{\infty} \frac{(-1)^k \tilde{\mathcal{P}}_n}{\mu_k^3}. \quad (39)$$

In the next section we will apply the analytical results obtained in this section to the case of active particles confined to a channel.

III. ACTIVE PARTICLES IN A CHANNEL

To verify the above analytical predictions, we consider now numerical simulations of particles confined to a channel, in which case we use $\theta_a = \pi/2$ in the above results. This case of a channel is practical since the two boundaries in this case prevent the particles from straying too far from the boundaries, which would made accumulating data slow. If the particles are initialized close to one of the two boundaries, memory effects from the initial conditions of the particle may
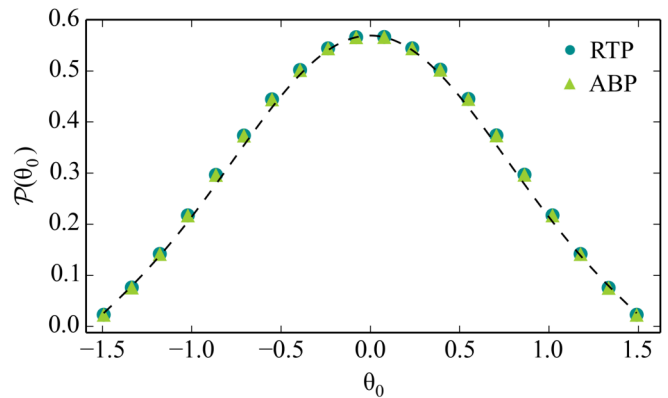

FIG. 5. Distribution of incoming angles $\mathcal{P}(\theta_0)$ for ABPs and RTPs from numerical simulations. We see that the two particle species have the same distribution, with only very minor differences. The black dashed line corresponds to the best fit of the two first Fourier modes as described in the text.

bias the simulation data. Here we restrict our attention to the case when the particles have spent a sufficiently long time in the bulk so that memory of the particles' initial conditions is lost. We therefore initialize the particles in the middle of the channel and assume that the channel half-width L is large compared to the persistence length $\tau_p v_0$ ($\tau_p = D_r^{-1}$ for ABPs, $\tau_p = \gamma^{-1}$ for RTPs).

A. The distribution of incoming angles

For ABPs originating far in the bulk hitting a flat boundary for the first time the distribution of incoming angles $\mathcal{P}(\theta_0)$ is expected to be maximal at $\theta_0 = 0$ and decay monotonically towards zero at $\theta_0 = \pm\pi/2$, as alluded to in the previous section. The monotonic decay is expected since the larger the particles' velocity component parallel to the boundary is, the more time noise has to act on its direction. Imagine an ABP close to a flat boundary. If noise reorients the particle away from the wall, there is no incoming angle to speak of, while if the noise reorients the particles to move towards the wall, the incoming angle would be closer to zero. Hence, finding incoming angles close to zero is the most likely. The same holds for RTPs, and the distribution of incoming angles is identical, as seen in Fig. 5.

From our derivations we know that the RTP case is insensitive to the incoming angle, while in the ABP case the distribution of incoming angles will affect the FPT distribution. In this case it will be useful to observe that $\mathcal{P}(\theta_0)$ is well approximated by the two first Fourier modes;

$$\mathcal{P}(\theta_0) \approx \tilde{\mathcal{P}}_0 \cos(\theta_0) + \tilde{\mathcal{P}}_1 \cos(3\theta_0). \quad (40)$$

From the numerical data, we find that $(\tilde{\mathcal{P}}_0, \tilde{\mathcal{P}}_1) = (0.508, 0.061)$ best fits the data, as shown in Fig. 5.

B. Trapping statistics

RTP case. As we have argued in previous sections, the run-and-tumble case has a universal exponentially decaying
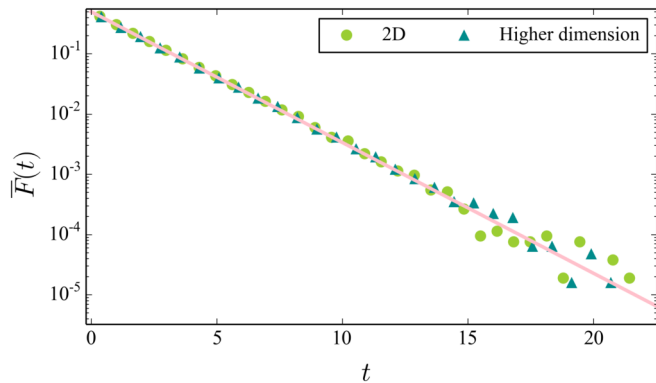
FIG. 6. FTP distribution for the run-and-tumble case, in units of the persistence time. Green circles result from numerical simulations of a 2D RTP as described in the dynamical equations. The dark blue triangles result from the simulation scheme of the higher-dimensional RTP as described in the text. As predicted, the trapping statistics is universal for all dimensions higher than 1, as shown by the pink solid line.
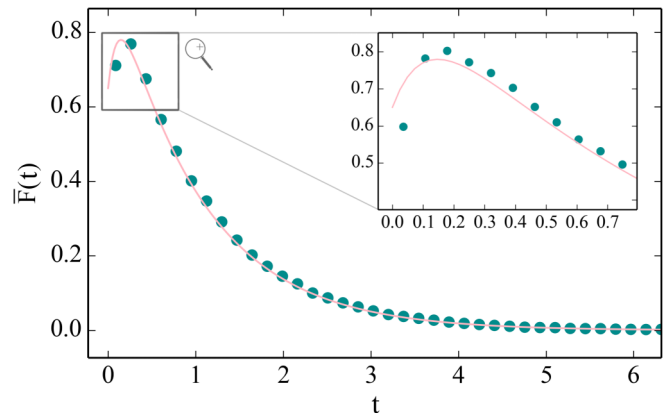

FIG. 7. Trapping time distribution for ABPs in units of the persistence time, obtained from simulations (dots) and semianalytical theory (solid line) based on numerically obtained parameters $\mathcal{P}_{0,1}$ for the distribution of incoming angles. The inset shows a close-up of the nonmonotonic behavior at early times.

first-passage time distribution in any dimension higher than 1, taking the form

$$\overline{F}(t) = F(t|\theta_0) = \frac{\gamma}{2} e^{-\gamma t/2}, \tag{41}$$

with no dependence on the incoming angle. The mean FPT is given simply by the tumbling rate $T_1 = \overline{T}_1 = 2/\gamma$. Figure 6 shows excellent agreement with this prediction of the numerical data for the trapping of run-and-tumble particles based on simulations of the dynamical equations (1). The higher-dimensional data were obtained as outlined at the end of Sec. II A.

ABP case. Using Eq. (38) for $\theta_a = \pi/2$ and keeping only the first two terms gives the collision-averaged FPT distribution

$$\frac{1}{D_r} \overline{F}\left(t, \frac{\pi}{2}\right) = 2\tilde{\mathcal{P}}_0 e^{-D_r t} - 6\tilde{\mathcal{P}}_1 e^{-9D_r t}. \tag{42}$$

If the distribution of incoming angles was a perfect cosine ($\tilde{\mathcal{P}}_1 = 0$), the trapping time distribution would simply be a pure exponential, and the mean trapping time would be the persistence time. Including the minor correction due to the second Fourier mode, we find the mean $\overline{T}_1 \approx 1.036$, in units of the persistence time. While this correction makes little difference to the numerical value of the mean trapping time, we see a clear effect of it in the trapping time distribution in Fig. 7, where the higher-order terms are responsible for the nonmonotonic behavior of the distribution for short trapping times. In other words, the likelihood of an ABP quickly escaping from the wall is highly sensitive to its incoming angle. By contract, particles that reside at the wall longer escape with a probability that is independent of the incoming angle and falls off exponentially with residence time.

IV. DISCUSSION AND OUTLOOK

In summary, we have studied the trapping statistics of active Brownian and run-and-tumble particles at flat solid boundaries. Since the escape from the wall is noise induced, we solved the first-passage problem associated with the angular dynamics of each particle type and found exact analytical expressions for the trapping time distribution. In the run-and-tumble case, the nature of the tumbling statistics makes the trapping time distribution independent of the incoming collision angle, while for the ABP case, the distribution depends strongly on the collision angle for short trapping times. We observe that both kinds of active particles have the same distribution of incoming angles, which is very well approximated by its two first cosine modes. This was used to calculate semianalytically the trapping time distribution averaged over incoming angles. The theoretical prediction agrees well with numerical simulations.

Several striking differences between the two species are observed. First, the trapping time distribution of ABPs is non-monotonic for short trapping times, while the RTP distribution is purely exponential. Furthermore, we argue that the obtained distribution in the RTP case is universal for any spatial dimension, which we verified for the three-dimensional case. The mean trapping duration for the ABP case is found to be close to 1.036 in units of the persistence time, while in the RTP case it is exactly 2. While it is well known that the dynamics of these two particle species are macroscopically equivalent in open spaces when using the same persistence time, here we showed a simple example of a discrepancy between the two models in the presence of boundaries.

While the distribution of incoming angles was found to be identical for both particle species, we should note that this will not be the case for the outgoing angle. In the RTP case, the escape angle is random and uniformly distributed, while ABPs will always leave the wall moving parallel to it. Throughout our analysis we have assumed that the particles are initialized sufficiently far from the wall so that any memory of initial conditions is lost. However, memory effects associated with multiple closely following trapping events is a case for further study, which may shed more light on the similarities and differences between ABPs and RTPs trapped at walls. In

this study, we have neglected alignment interactions between active particles as well as any hydrodynamic effects, which are important for the wall accumulation phenomenon. Thus, it would be interesting to study further their role in the wall-trapping statistics.

[1] Y. B. Dor, S. Ro, Y. Kafri, M. Kardar, and J. Tailleur, Disordered boundaries destroy bulk phase separation in scalar active matter, Phys. Rev. E **105**, 044603 (2022).

[2] H. Jiang, H. Ding, M. Pu, and Z. Hou, Emergence of collective dynamical chirality for achiral active particles, Soft Matter **13**, 836 (2017).

[3] K. S. Olsen, L. Angheluta, and E. G. Flekkøy, Escape problem for active particles confined to a disk, Phys. Rev. Res. **2**, 043314 (2020).

[4] L. Caprini and U. M. B. Marconi, Active chiral particles under confinement: Surface currents and bulk accumulation phenomena, Soft Matter **15**, 2627 (2019).

[5] C. F. Lee, Active particles under confinement: Aggregation at the wall and gradient formation inside a channel, New J. Phys. **15**, 055007 (2013).

[6] J. Elgeti and G. Gompper, Wall accumulation of self-propelled spheres, Europhys. Lett. **101**, 48003 (2013).

[7] M. E. Cates and J. Tailleur, When are active Brownian particles and run-and-tumble particles equivalent? Consequences for motility-induced phase separation, Europhys. Lett. **101**, 20010 (2013).

[8] A. P. Solon, M. E. Cates, and J. Tailleur, Active Brownian particles and run-and-tumble particles: A comparative study, Eur. Phys. J.: Spec. Top. **224**, 1231 (2015).

[9] M. Khatami, K. Wolff, O. Pohl, M. R. Ejtehadi, and H. Stark, Active Brownian particles and run-and-tumble particles separate inside a maze, Sci. Rep. **6**, 37670 (2016).

[10] G. Junot, T. Darnige, A. Lindner, V. A. Martinez, J. Arlt, A. Dawson, W. C. K. Poon, H. Auradou, and E. Clément, Run-to-Tumble Variability Controls the Surface Residence Times of *E. coli* Bacteria, Phys. Rev. Lett. **128**, 248101 (2022).

[11] K. Schaar, A. Zöttl, and H. Stark, Detention Times of Microswimmers Close to Surfaces: Influence of Hydrodynamic Interactions and Noise, Phys. Rev. Lett. **115**, 038101 (2015).

[12] É. Fodor and M. C. Marchetti, The statistical physics of active matter: From self-catalytic colloids to living cells, Phys. A (Amsterdam, Neth.) **504**, 106 (2018).

[13] J. Elgeti and G. Gompper, Microswimmers near surfaces, Eur. Phys. J.: Spec. Top. **225**, 2333 (2016).

[14] J. Elgeti and G. Gompper, Self-propelled rods near surfaces, Europhys. Lett. **85**, 38002 (2009).

[15] V. Kantsler, J. Dunkel, M. Polin, and R. E. Goldstein, Ciliary contact interactions dominate surface scattering of swimming eukaryotes, Proc. Natl. Acad. Sci. USA **110**, 1187 (2013).

[16] E. Lushi, V. Kantsler, and R. E. Goldstein, Scattering of biflagellate microswimmers from surfaces, Phys. Rev. E **96**, 023102 (2017).

[17] S. Redner, *A Guide to First-Passage Processes* (Cambridge University Press, Cambridge, 2001).

[18] B. Besga, F. Faisant, A. Petrosyan, S. Ciliberto, and S. N. Majumdar, Dynamical phase transition in the first-passage probability of a Brownian motion, Phys. Rev. E **104**, L012102 (2021).

[19] G. Pozzoli and B. De Bruyne, Survival probability of random walks leaping over traps, J. Stat. Mech. (2021) 123203.

[20] D. A. Darling and A. Siegert, The first passage problem for a continuous Markov process, Ann. Math. Stat. **24**, 624 (1953).

[21] A. J. Bray, S. N. Majumdar, and G. Schehr, Persistence and first-passage properties in nonequilibrium systems, Adv. Phys. **62**, 225 (2013).

[22] A. Pal and V. V. Prasad, First passage under stochastic resetting in an interval, Phys. Rev. E **99**, 032123 (2019).

[23] A. Pal, I. P. Castillo, and A. Kundu, Motion of a Brownian particle in the presence of reactive boundaries, Phys. Rev. E **100**, 042128 (2019).

[24] S. Redner, A first look at first-passage processes, arXiv:2201.10048.

[25] R. Zwanzig, *Nonequilibrium Statistical Mechanics* (Oxford University Press, Oxford, 2001).

[26] E. T. Whittaker and G. N. Watson, *A Course of Modern Analysis* (Cambridge University Press, Cambridge, 1996).